

1-30-2013

Satellite imagery evaluation of soil moisture variability in north-east part of Ganges Basin, India

Proma Bhattacharyya

Follow this and additional works at: https://digitalrepository.unm.edu/eps_etds

Recommended Citation

Bhattacharyya, Proma. "Satellite imagery evaluation of soil moisture variability in north-east part of Ganges Basin, India." (2013).
https://digitalrepository.unm.edu/eps_etds/6

This Thesis is brought to you for free and open access by the Electronic Theses and Dissertations at UNM Digital Repository. It has been accepted for inclusion in Earth and Planetary Sciences ETDs by an authorized administrator of UNM Digital Repository. For more information, please contact disc@unm.edu.

Proma Bhattacharyya

Candidate

Earth and Planetary Sciences

Department

This thesis is approved, and it is acceptable in quality and form for publication:

Approved by the Thesis Committee:

Gary Weissmann

, Chairperson

Louis Schuderi

Grant Meyer

Satellite Imagery Evaluation of Soil Moisture Variability in
North-East part of Ganges Basin, India

By

Proma Bhattacharyya

B.Sc Geology, University of Calcutta, India, 2007

M.Sc Applied Geology, Presidency College-University of Calcutta, 2009

THESIS

Submitted in Partial Fulfillment of the
Requirements for the Degree of
Master of Science
Earth and Planetary Sciences

The University of New Mexico, Albuquerque, New Mexico

Graduation Date – December 2012

ACKNOWLEDGMENTS

I heartily acknowledge Dr. Gary W. Weissmann, my advisor and dissertation chair, for continuing to encourage me through the years of my MS here in the University of New Mexico. His guidance will remain with me as I continue my career. I also thank my committee members, Dr. Louis Scuderi and Dr. Grant Meyer for their valuable recommendations pertaining to this study. To my parents and my fiancé, thank you for the many years of support. Your encouragement is greatly appreciated.

Satellite Imagery Evaluation of Soil Moisture Variability in North-East part of Ganges Basin, India

Proma Bhattacharyya

B.Sc Geology, University of Calcutta, India, 2007

M.Sc Applied Geology, Presidency College-University of Calcutta, 2009

ABSTRACT

Soil moisture variability across four river systems in Ganges Basin, from the Tista and Kosi Rivers in the east to the Gandak and Ghaghra-Rapti Rivers in the west, was assessed using Landsat TM Band 6 imagery dating from 1999-2003. The Band 6 thermal channel of Landsat is sensitive to soil temperature variability resulting from differences in moisture content and as such is a proxy for soil moisture variability in this environment. In order to take advantage of this relationship we analyzed the imagery focusing on the range of thermal values across the fans. This range calculation separates seasonally dry and perennially wet soils on the basis of variability in their moisture content throughout the year. Soils that have a high range (high variability) show significant drying after the monsoon, while those that exhibit a low range indicate either constant wet or dry conditions and/or vegetation that does not vary seasonally. Ground based assessments of soil characteristics on the Tista and Kosi fans support this image analysis. Our work, supported by literature, indicates that the Tista DFS (Distributive Fluvial System) and the Ghaghra-Rapti interfluvium, where river is currently incised and detached from its floodplain, show an increase in soil moisture content downstream. However, the Kosi and Gandak DFSs, which have higher rate of subsidence and are not incised under current climatic conditions, show no trend in soil moisture distribution. This study indicates that degree of incision and water table depth are important controls for soil moisture distribution across the DFSs in this area.

Table of Content

Chapter I – Introduction	1
Chapter II – The Manuscript	2
1 Introduction	2
2 Study Area	5
2.1 Climate	5
2.2 Large DFSs in the study area	6
2.2.1 Tista DFS	8
2.2.2 Kosi DFS	9
2.2.3 Gandak DFS	10
2.2.4 Ghaghara-Rapti incised DFS	11
3 Methodology	13
3.1 Range Statistics	13
3.2 Maximum Likelihood Classification	14
4 Analysis and Interpretation	15
4.1 Tista DFS	15
4.2 Kosi and Gandak DFS	18
4.3 Ghaghra-Rapti incised DFS	21
5 Discussion	23
5.1 Degree of Incision	23
5.2 Depth to Water Table	24
5.3 Climate	25
6 Future Work	25
7 Conclusions	26
Chapter III – Appendix	27
A1 – Detail Methodology	27
A2 – Supplementary Figures	S1

List of Figures

Figure 1: The study area	3
Figure 2: Average annual rainfall distribution in India	6
Figure 3: A shaded relief map of the Ganges Plain, India	8
Figure 4a: A Google Earth image of the Tista DFS	9
Figure 4b: A Google Earth image of the Kosi DFS	10
Figure 4c: A Google Earth image of the Gandak DFS	11
Figure 4d: A Google Earth image of the Ghaghra-Rapti incised DFS	12
Figure 5: The Geomorphic subdivisions of the Ghaghra-Rapti incised DFS and the Gandak DFS	13
Figure 6: A map of the range statistic results for the study area	14
Figure 7: The maximum likelihood classification of the Tista DFS	16
Figure 8: Range statistics of Tista DFS	17
Figure 9: Photographs of deposits in the proximal portions of the DFS	18
Figure 10: Photographs from the medial Tista DFS	19
Figure 11: Photographs from the Distal Tista DFS	20
Figure 12: Range statistics for the Kosi DFS and the Gandak DFS	20
Figure 13: Three cross-profiles of Kosi DFS	21
Figure 14: The Dartmouth Floodmap (http://www.dartmouth.edu/~floods/hydrography/E80N30.html)	22
Figure 15: Photographs of soils and landscape on the distal Kosi DFS	22
Figure 16: Range statistics and SRTM of the Ghaghra DFS	23

Chapter I - Introduction

Soil moisture variation across four Distributive Fluvial Systems (DFS) is the main point of interest of this thesis. This thesis starts with this introduction followed by a manuscript and an Appendix. The manuscript is in preparation for publishing in the International Journal of Remote Sensing. The Appendix contains several supporting figures and detailed methodology. The methodology section includes commands that were used in ArcMap and in Matlab for future reference mostly. All of these methods are not directly related to my study however, they were used to process images. Therefore all of them have not been mentioned in the main text.

Chapter II – Manuscript

1. INTRODUCTION

Soils are important elements in reconstructing geomorphic history and they directly influence other surficial processes (Ritter et al. 2006). Soil moisture is an important factor that determines energy exchanges between the land and the atmosphere (Wang et al. 2010), the spatial and temporal dynamics of terrestrial eco-systems (Carlson, 1994; Zhiming et al. 2007) and water available for evaporation from the land surface and agriculture (Wang et al. 2010). It has been recognized that soil moisture variability down a Distributive Fluvial System (DFS), where a DFS is defined as “*the deposit of a fluvial system which in planform displays a radial, distributive channel pattern*” (Hartley et al. 2010), could be an important characteristic of these landforms (Hartley et al. *in press*; Weissmann et al. *in press*).

Analysis to determine soil moisture in the field and laboratory with precision is expensive and time consuming. Therefore researchers have used remote sensing tools to analyze soil moisture over large areas. For example, Carlson et al. (1994) estimated surface soil moisture availability in the presence of variable vegetation cover. They used a model that coupled a Soil-Vegetation-Atmosphere-Transfer and Normalized Vegetation Difference Index. Their results of surface soil moisture availability and fractional vegetation cover were qualitatively realistic. However, Carlson (1994) himself has mentioned that the distribution of soil moisture availability was questionable at high fractional vegetation amounts. Gillies et al. (1997) developed a model for determining surface water content, fractional vegetation cover and the instantaneous surface energy fluxes using remotely sensed data derived from the NS001 multispectral scanner carried on board NASA’s C-130 aircraft. Nanni et al. (2006) successfully evaluated the question, whether soil attributes, such as clay, sand and TiO_2 , Fe_2O_3 content can be studied by remote sensing methodology instead of physical-chemical analysis. They normalized Landsat digital images such

that they could compare with the spectral reflectance value of attributes of soil components. Wang et al. (2010) used thermal infrared Landsat TM images and produced a land use and cover type map and they used it to study the influence of land use and cover type changes on soil moisture.

In this paper, a time-series of Landsat band 6 thermal data from Landsat scenes of the part of Ganges Basin was used to evaluate the spatial and temporal soil moisture distribution pattern across four DFSs which are located in different depositional regimes (Figure 1).

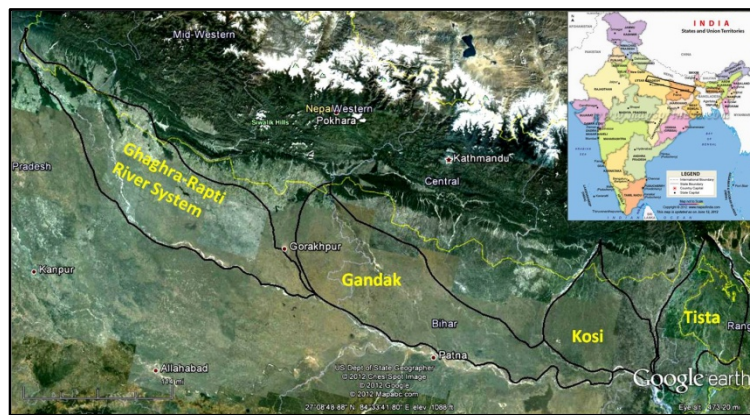


Figure 2: The study area, showing the Tista, Kosi, and Gandak DFS and the Ghaghra-Rapti incised DFS in the northern part of the Ganges Basin, located in northern India. The DFSs are separated from each other by smaller DFS in the interfan zones (Image from Google Earth).

I used Landsat Band 6 thermal data that record the emissivity of the land surface. Emissivity describes how efficiently an object radiates thermal radiation (Shaw et al. 2000). A perfect blackbody would have highest emissivity i.e. 1, as it reflects nothing (Shaw et al. 2000). The emissivity value of water is close to that of Blackbody's ~ 0.98 (<http://www.infrared-thermography.com/material-1.htm>). Mira et al. (2007) noted a common increase of emissivity of soil with soil water content. They determined moisture content of different soil types in laboratory using gravimetric method and measured emissivity of them with two-lid variant of the box method. The result shows that due to adhered water particles reflectivity of soil decreases which in turn increases soil emissivity. Wang et al. (2010) also noted that with increasing soil moisture content soil reflectance decreases i.e. emissivity increases (Zhiming et al. 2006). This

relationship between the emissivity and soil moisture content is the basis of this current study as the thermal bands have been used here as a proxy for soil moisture content. However, in highly vegetated areas land surface emissivity recorded by remote sensing, actually represent vegetation canopy's emissivity. Cloud-free Landsat scenes were obtained to create a time series of images between 1999 and 2003 (Table 1) to study the range of seasonal variation in soil moisture content. I studied deposits of four river systems of the Ganges Basin -- the Tista, the Kosi, the Gandak, and the Rapti-Ghaghara DFS, from east to west, respectively (Figure 1). The soil moisture distribution patterns are not similar in all the river systems. In this paper I will start with description of the study area, methodology, analysis and interpretation followed by a discussion and conclusion.

Months	p139r042	p140r042	p141r041	p141r042	p142r041	p142r042	p143r041	p143042	p144r040	p144r041
January	2001	2002		2001						
February	2000	2001, 2003	2001	2003	2000, 2002	2002, 2003	2000, 2001, 2001, 2001	2000, 2000, 2001, 2003	2000, 2002, 2003	2000, 2002, 2003
March	2002, 2003	2000, 2001, 2002	2003	2000, 2001, 2002, 2003	2003	2003		2000, 2002, 2003		2001
April				2003	2001, 2002, 2003	2000	2001	2001	1999, 2000, 2002, 2003	2000, 2002, 2003
May		2002	2002	2002		2002, 2003	2000		2000	2001
June				2002			2002	2002		2000, 2002
July										2002
August										
September					2000	2000		2001		2000, 2001, 2002
October	2002	1999, 2000, 2002	2001	2000, 2001	1999	1999, 2001	1999, 2000, 2002	1999, 2000, 2002	2000, 2002	
November	1999	1999	1999, 2000, 2002	1999, 2000, 2002	2002		2000	2000	2001, 2002	1999, 2000, 2001, 2002
December	2000, 2001	2000, 2002		2000, 2001	1999	1999, 2000	1999, 2001	1999, 2002		1999, 2000

Table 1: Time series of Band 6 data for each path-row showing available data used for this study

2. STUDY AREA

The study area covers the northeastern part of the Ganges Basin portion of the Himalayan foreland basin and includes part of the states of Uttar Pradesh, Bihar and West Bengal in India and some parts of Bangladesh and Nepal (Figure 1). This foreland basin developed as a result of collision of the India and Asia continental plates during the Paleocene, and the basin is still actively subsiding (Mohindra et al. 1994; Sinha et al. 2005). However, the subsidence rate is not equal throughout the study area (Pati et al. 2011). Tista DFS and Ghaghra-Rapti incised DFS is marked by lesser subsidence compared to Kosi and Gandak DFSs (Pati et al. 2011). This study indicates that tectonics is one of the important factors controlling soil moisture distribution throughout these DFSs.

2.1 Climate

The southwest Indian monsoon exerts a dominating influence on the Ganges Plains (Tandon et al. 2006). In general the western part of the Ganges Basin receives less rainfall (100-120cm) than the eastern part (160-200cm) (Pati et al. 2011) (Figure 2.a). Figures 2.b and 2.c show the annual distribution of rainfall in Darjeeling and Lucknow. These cities are situated in the eastern and western part of the study area respectively. These figures show that monsoon arrives in this area in mid-June and lasts through August. Due to this pattern, soils that are dry throughout much of the year become saturated during the monsoon rains however, wet soils remain saturated during the dry season. In this study seasonal variation in soil moisture in dry soils was used to compare it with wet soils.

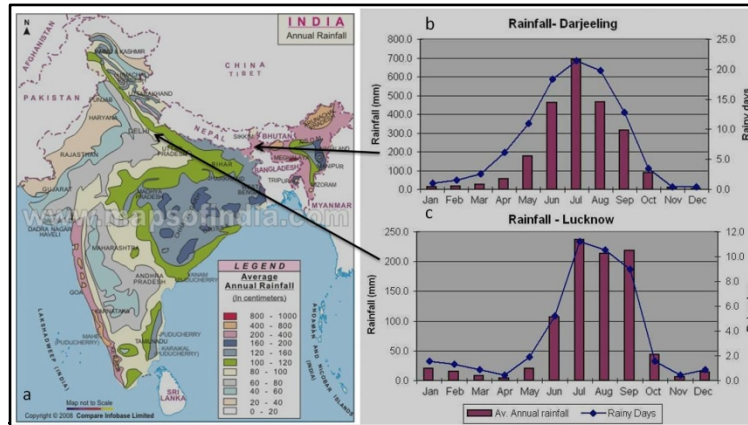


Figure 2a: Average annual rainfall distribution in India; b: Average annual rainfall distribution in Darjeeling, India, close to Tista DFS; c: Average annual rainfall distribution in Lucknow, India, close to Ghaghra DFS

2.2 Large DFSs in the Study area

A DFS can be recognized by a radial pattern of channels from the DFS apex, decreasing grain size and channel size down-slope and lack of lateral channel confinement (Weissmann et al. 2010). All of these are prominent in Tista, Kosi and Gandak DFSs. In current climatic condition these conditions are not apparent in Ghaghra-Rapti system. Therefore, according to Fielding et al. (2012) Ghaghra_Rapti system should not be considered as a DFS as it is presently incised. However, Weissmann et al. (2002, 2005) has shown that with changing climatic condition rate of incision of a river varies in time depending on the rate of sediment and water discharge. Due to high sediment discharge during the aggradational period large DFSs are formed. With increasing water supply during the degradational period rivers start to incise into this DFS. Mohindra et al. (1994) has documented meander scars on Ghaghra DFS. Presence of these paleochannels indicates that Ghaghra and Rapti were distributive during the aggradation period.

Srivastava et al. (1994) classified the Ganges plain into three parts -- the Upper, Middle and Lower Ganges plain -- based on their morphological and hydrological features. The Upper Ganges Plain is characterized by uplands with incised rivers. The Middle Ganges Plain is marked by higher rates of subsidence and rivers that are not incised. The Lower Ganges Plain is dominated by deltaic activity (Pati et al. 2011). The Ghaghra-Rapti incised DFSs are located in

Upper Ganges Plain and The Kosi and Gandak DFS are part of the Middle Ganges plains (Srivastava et al. 1994) (Figure 3). Though the Tista DFS is classified in the Lower Ganges Plain region, it is not influenced by deltaic activity. Based on the source area characteristic Sinha et al. (1994) has classified the river systems in the Himalayan foreland basin into three classes -- mountain-fed, foothills-fed and plains-fed rivers. Mountain-fed rivers, such as Gandak and Kosi, are characterized by a large upland source area, a high ratio of upland source area to plains and a high discharge (Sinha et al. 1994). The Baghmata River, located in the interfan area between Kosi and Gandak, is an example of foothills-fed rivers (Sinha et al. 1994). These rivers are characterized by a much lower ratio of upland source area to

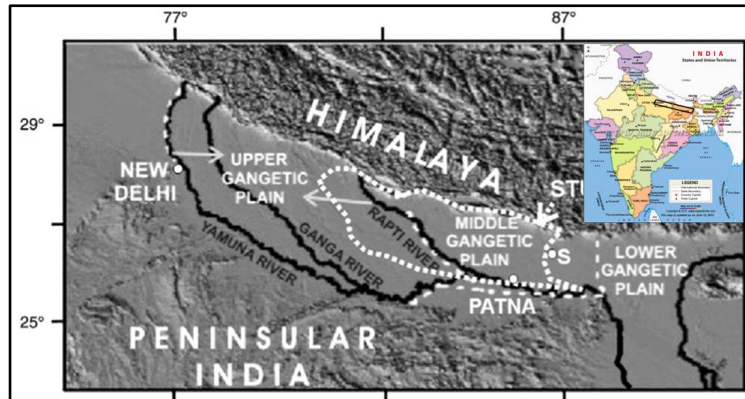


Figure 3: A shaded relief map of the Upper, Middle, and lower Ganges Plain with subdivisions of the Ganges Plain according to the patterns of deposition (From Srivastava et al. 1994).

alluvial area along with a smaller discharge. Plains-fed rivers or groundwater-fed rivers (Gohain et al. 1990) are entirely confined to the alluvial plains and therefore having an upland source area to alluvial area ratio of zero. The modern channels present on Tista DFS are example of plains-fed rivers. Sedimentation on the modern depositional surface of the Ganges basin is dominated by fluvial megafans (Gupta, 1997). The four fluvial megafans/DFSs, from east to west, namely Tista, Kosi, Gandak, Rapti and Ghaghra, constitute point-sourced depositional systems and are separated from each other by broad interfan areas (Gupta, 1997) (Figure 1). The main features of the studied DFSs are described below.

2.2.1 Tista DFS – The Tista DFS, the eastern-most DFS in the study area (Figure 4a), spreads across the state of West Bengal in India and Bangladesh and covers an area of 18,000 km² (Chakraborty et al. 2010a). The average annual discharge between 1965 and 1971 is about 609m³/s ([www.sage.wisc.edu/riverdata/scripts/station_table.php? qual=32& filenum = 2567](http://www.sage.wisc.edu/riverdata/scripts/station_table.php?qual=32&filenum=2567)) (Chakraborty et al. 2010a). This DFS is a large triangular sedimentary body bounded by the Mahananda River to the west. Its eastern margin broadly coincides with the modern Tista River (Figure 4a). During a major flood in 1787,

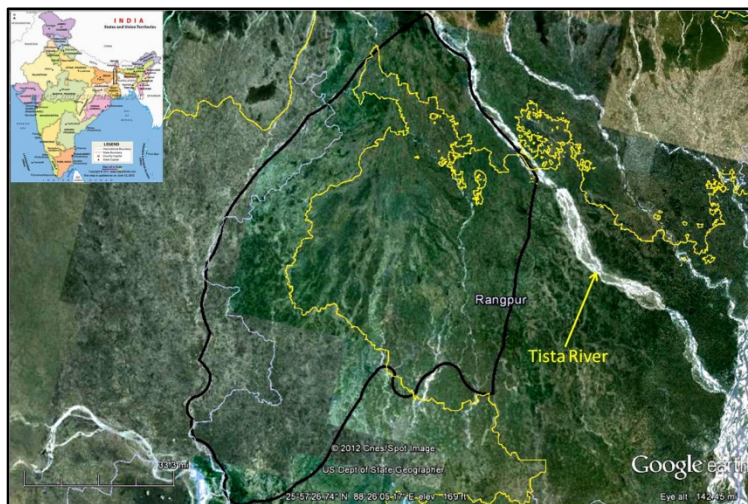


Figure 4a: A Google Earth image of the Tista DFS. This DFS covers portions of West Bengal, India and Bangladesh. the Tista River avulsed into its present-day course of Tista abandoning this older DFS surface (Hunter 1876; Ray 1980; Chakraborty et al. 2010a), though the exact location of this avulsion is unclear from satellite imagery. Chakraborty et al. (2010a) have reported that there are a large number of paleochannels and modern channels that traverse this DFS. Modern plains-fed channels are incised and they have higher sinuosity and lower width compared to the paleochannels (Chakraborty et al. 2010a). However, there is an increase in sinuosity of both modern and past channels down the DFS. This DFS has multi-lobate character (Chakraborty et al. 2010a).

2.2.2 Kosi DFS – West of the Mahananda interfan area, the Kosi DFS spreads across portions of Nepal and the state Bihar in India (Figure 4b). The present Kosi channel belt flows along a curved path around the western edge of the Kosi DFS, ultimately turning eastward sub-parallel to the Ganga, which it ultimately joins (Figure 4b). The Kosi DFS covers an approximately 10,351 km² area. The Average monthly discharge of the Kosi River varies from >6000m³/s to 500m³/s (Chakraborty et al. 2010b). Several authors describe a continuous westward migration of the Kosi River across its DFS over the last



Figure 4b: A Google Earth image of the Kosi DFS, located in the northern portion of Bihar, India, and southern Nepal. two centuries (Mookerjee 1961; Mookerjee et al. 1963; Gole et al. 1966; Wells et al. 1987; Gohain et al. 1990; Duff 1992; Singh et al. 1993; Mackey et al. 1995; Collinson 1996; Decelles et al. 1999; Bridge 2003; Assine 2005). However, Chakraborty et al. (2010b) used historical records to propose that the Kosi River has avulsed in a non-systematic manner instead of a constant westward migration. Similar to the Tista DFS, a number of modern and ancient channels have been reported on the Kosi DFS. Their study was based on 28 historical maps, published between 1760-1960, and fieldwork. These modern plain-fed channels are incised and they are more

sinuous and narrower than the paleochannels. However, both the Kosi modern and ancient channels show increase in their sinuosity down the DFS. The Kosi River is not incised into its DFS and has recently (in 2008) flooded much of the DFS surface (Sinha et al. 2005).

The Kosi DFS is located in between two interfan areas. The Mahananda interfan, situated between Tista and Kosi DFS, is occupied by stream-dominated alluvial fans in their proximal part and mainly meandering rivers and associated floodplains with oxbows and sloughs in their downstream parts (Figure 1). Another interfan area is present between the Kosi DFS and the Gandak DFS that contains numerous smaller fans (Figure 1). The Burhi Gandak, Bagmathi, Kamla and Balan Rivers form some of the larger DFS in this interfan area ((Sinha et al. 1994; Pati et al. 2011). Among these streams, the Baghmati River is considered to be hyperavulsive (Sinha et al. 2003). Sinha et al. (2003) reported eight major and several minor avulsion events of Baghmati River in last 230 years.

2.2.3 Gandak DFS: The Gandak River formed this DFS in parts of Nepal and in the states of Bihar and Uttarpradesh in India (Figure 4c).

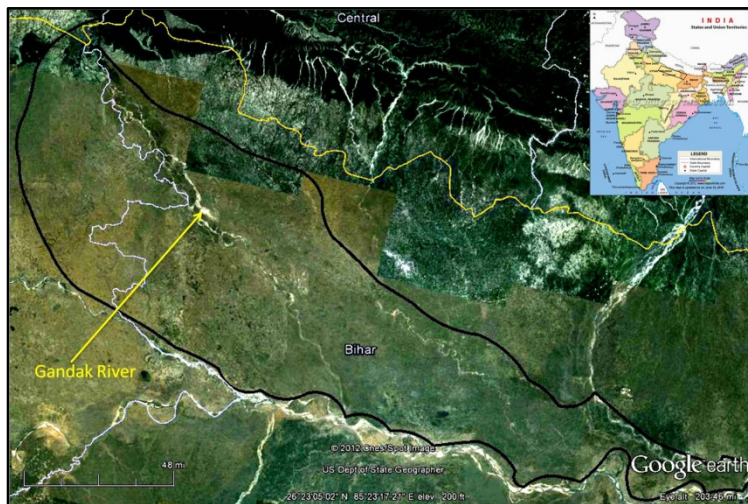


Figure 4c: A Google Earth image of the Gandak DFS, located in the the states of Bihar and Uttarpradesh, India, and southern Nepal.

The Gandak DFS is located between two interfan areas (Figure 1). The Gandak DFS has an elongated form trending northwest-southeast and covers an area of about 27,500 km² (Mohindra et al. 1994) (Figure 4c). The Gandak River is braided in the proximal and medial portion of its DFS; however it becomes straight in the distal reaches (Mohindra et al. 1994). The Gandak River has shifted about 105km eastward due to tectonic tilting (Mohindra et al. 1994). The abandoned paleochannels are now occupied by small groundwater-fed streams like Rohini, Bensi, and Jharahi Rivers (Mohindra et al. 1994). The Gandak DFS is comprised of the Gandak River floodplain area along the middle of the DFS, the Young Gandak Plain, and the Old Gandak Plain (Mohindra et al. 1992). Pati et al. (2010) described these Young Gandak Plains as terminal fans (Figure 5). On these terminal fans there are a number of sandy ridges with a slightly raised level and low lying paleochannels alternating with these sandy ridges marked by linear alignment of ponds in some of these terminal fans (Pati et al. 2010). In this study I will follow Mohindra et al. (1992) terminology and consider the Pati et al. (2010) terminal fans to be lobes of deposition on the DFS.

2.2.4 Ghaghara-Rapti Incised DFS: The Ghaghara-Rapti river system is part of the

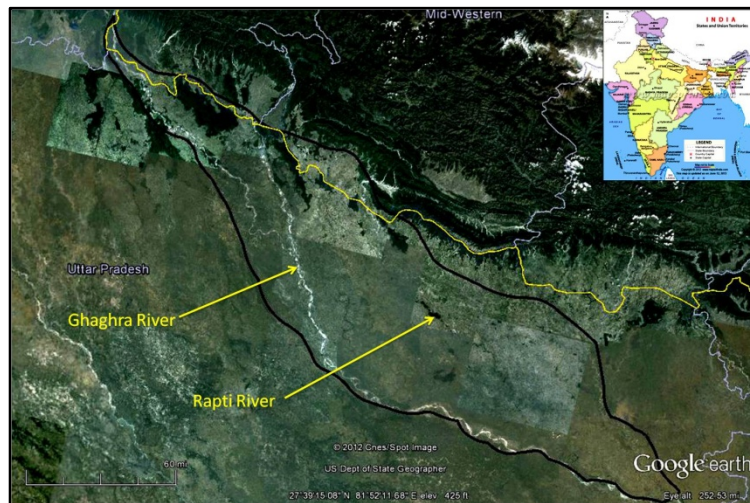


Figure 4d: A Google Earth image of the Ghaghara-Rapti incised DFS, located in parts of southern Nepal and the Uttarpradesh State of India.

Upper Ganges Plain (Srivastava 1994) (Figure 3). It is situated in parts of Nepal and the Uttarpradesh state of India (Figure 4d). It consists of a Piedmont zone, Rapti Floodplain, the Rapti Terminal fans, Ghaghra-Rapti interfluvium, Old Ghaghra Plain and Ghaghra Floodplains and terraces (Pati et al. 2010) (Figure 5). The piedmont zone consists of

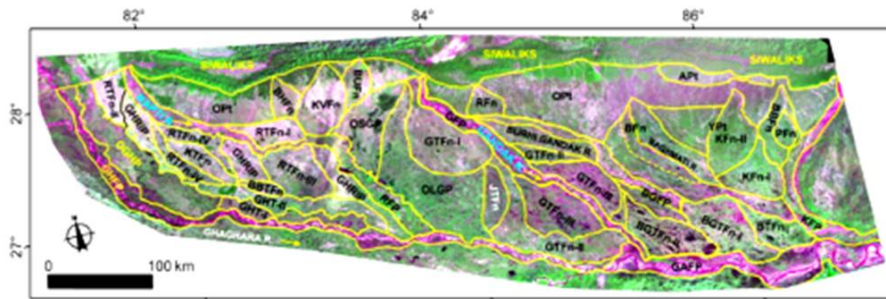


Figure 5: The Geomorphic subdivisions of the Ghaghra-Rapti incised DFS and the Gandak DFS (from Pati et al., 2010). Abbreviations ending with TFn, Fn, T-I/T-II, P, FP, and Pt refer to terminal fans, fans, terraces, plains, floodplains and piedmont, respectively. Abbreviations used for various terrain morphologicals are given below. Piedmont zone in the whole area: APt: Active Piedmont (including BFn: Baghmata Fan and KFn-I: Kamla Fan I); YPt: Young Piedmont (including KFn-II: Kamla Fan II, and PFn: Phulparas Fan); OPt: Old Piedmont (including BHF: Bahadurgarh Fan; KVFn: Kapilvastu Fan; BuFn: Butwal Fan; BBFn: Bhatibalan Fan and RFn: Ramnagar Fan). Ghaghra-Rapti area: RFP: Rapti Floodplain; GHFP: Ghaghara Floodplain; Rapti Terminal Fan I; RTFn-II; Rapti Terminal Fan II; RTFn-III: Rapti Terminal Fan III; RTFn-IV: Rapti Terminal Fan IV, KTFn: Khujurpur Terminal Fan, and BBTFn: Babbaan Terminal Fan; GHT-I: Ghaghara Terrace I; GHT-II: Ghaghara Terrace II; GHRIP: Ghaghara-Rapti Interfluvium Plain; OGHP: Old Ghaghara Plain. Rapti-Gandak area: GTFn-I: Gandak Terminal Fan I; GTFn-II: Gandak Terminal Fan II; GTFn-III: Gandak Terminal Fan III; JTFn: Jharani Terminal Fan, GAFP: Ganga Floodplain, GFP: Gandak Floodplain; OSGP: Oldest Gandak Plain, and OLGP: Old Gandak Plain. Gandak-Kosi area: BTFn: Baghmata Terminal Fan, BGTFn-I: Burhi Gandak Terminal Fan I; BGTFn-II: Burhi Gandak Terminal Fan II; BTFn: Baghma Terminal Fan, and BGFP Burhi Gandak Floodplain.

coarse sand and gravels (Pati et al. 2010). The young Ghaghara and Rapti floodplains have an elongated form, trending northwest southeast (Figure 4d). The area marked as Rapti terminal fans by Pati et al. (2010) is situated between Old Ghaghra Plain and Rapti floodplains and thus in this study it is included in Rapti-Ghaghara interfluvium (Figures 4d and 5). This area is elevated (Pati et al. 2011) (Figure 5). Pati et al. (2011) identified terraces on this river system, however these appear to be abandoned depositional lobes on these DFS (Figure 5). These terraces are characterized by coarse sand deposits (Pati et al. 2010).

3. METHODOLOGY

I used two approaches to analyze the seasonal variability and spatial distribution pattern of soil moisture content with the time series data, including assessment of seasonal thermal signal (band 6) ranges of the entire study area and a maximum likelihood classification of the thermal signal from the Tista DFS. All analyses were conducted in the ArcGIS platform (ver. 9.3, ESRI 2009).

3.1 Range Statistics: Range statistics of a time series represents the difference between maximum and minimum value for each cell within a given time period. I evaluated thermal range value observed throughout the year across each DFS on cell-by-cell basis (Figure 6).

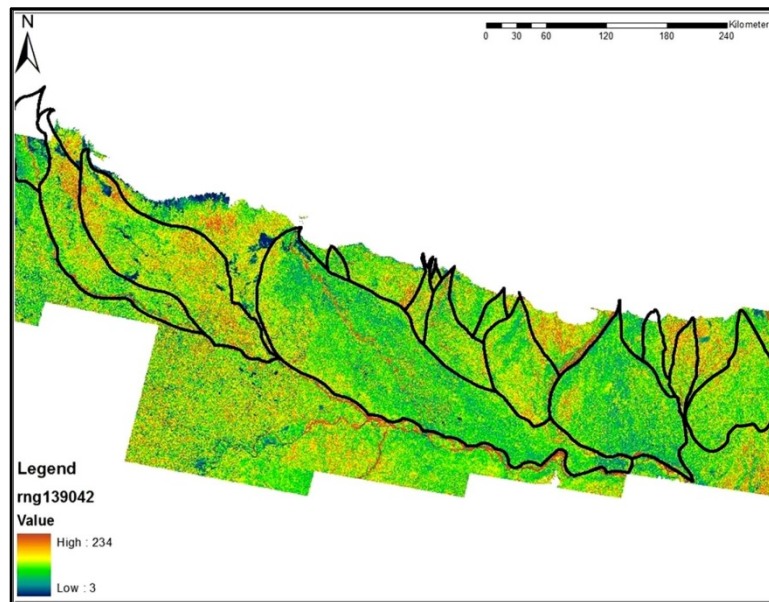


Figure 6: A map of the range statistic results for the study area. The black outlines mark the major DFS boundaries. Drier regions with relatively well-drained soils have dry soils all throughout the year except during the monsoon (June-August), when the soil will be saturated with the water due to flooding and high rainfall. Therefore, areas with large range will be those that exhibit significant drying throughout the year, with the wet phase occurring during the monsoon. Conversely, areas with low range values reflect consistent moisture levels throughout the year (e.g., areas that remain relatively wet throughout the year). River channels always give high range values. During

monsoon, channels get filled up with water however, in dry season there is less water and channel belt deposits become exposed. Therefore they show high variability in thermal emissivity signal. Evergreen vegetation canopy (e.g., trees and tea plantations) will have a relatively constant thermal value throughout the year in band 6 images. Therefore the seasonal range of thermal signal in these vegetated areas would be low. If the underlying soil is originally dry, then presence of dense vegetation could be misleading.

3.2 Maximum Likelihood Classification: The maximum likelihood (ML) classifier calculates the probability of a pixel belonging to each of a pre-defined set of M classes and then assigns that to the class for which the probability is the highest (Jensen, 2006). The classes are defined on the basis of prior knowledge, which in this case are field observations and existing literature. This supervised classification scheme was used to classify the time series data of Tista DFS into seven classes according to the thermal signal of each pixel (Figure 7a). A majority filter was applied to the resultant classified image in order to clean up the map by removing noise across this DFS (Figure 7b). A majority filter replaces cells in an image based on the majority of their contiguous neighboring cells.

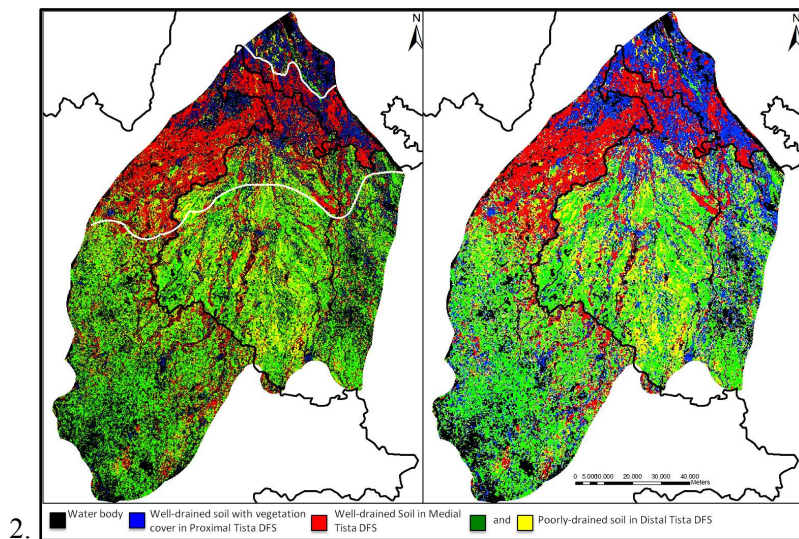


Figure 7a: The maximum likelihood classification of the Tista DFS. White lines outline the boundaries of the three zones -- proximal, medial, and distal, classified according to the soil moisture variability. b: The Maximum Likelihood results after smoothing with a majority filter.

These thermal data were used in conjunction with the elevation data derived from the Shuttle Radar Topography Mission (SRTM), Dartmouth Flood Observatory maps (<http://www.dartmouth.edu/~floods/hydrography/E80N30.html>) and field observations of soil character and general geomorphology. SRTM images were commonly used to understand the relative degree of incision of the studied rivers. A field survey was conducted along a down-DFS transect on the Tista DFS in West Bengal, India, and on the distal portion of the Kosi DFS in Bihar, India during January, 2011. Down-DFS changes in soil type and vegetation pattern were noted in this field survey in order to serve as ground truth for the interpretations from image analysis.

4. ANALYSIS AND INTERPRETATIONS

4.1 Tista DFS

In the resultant image of the range calculation, low range values are observed at the apex, with higher values in the medial portions of the DFS and lower values distally (Figure 8). This zonation was also documented within the ML classified image (Figures 7a and b).

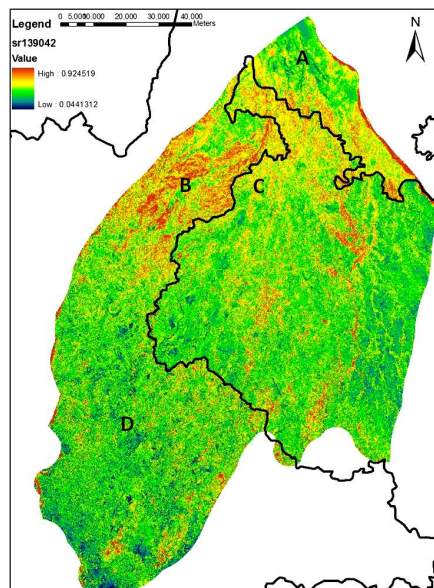


Figure 8: Range statistics of Tista DFS. A - Low range value in the proximal part; B - High range value at the middle part; C - Decreasing range value across India-Bangladesh border; D - Low range values in distal part

A sharp change in the thermal variability signature is observed in the medial part of Tista DFS along India-Bangladesh border, with the Bangladesh portion of the medial Tista DFS displaying lower range values than those in India (Figure 8). The NDVI analyses were unable to show differences vegetation between the proximal and distal part of this DFS (Figure A3d and Figure A3f). This sharp difference in thermal signature, however, is probably anthropogenic in origin since it falls directly on the border between these two countries.

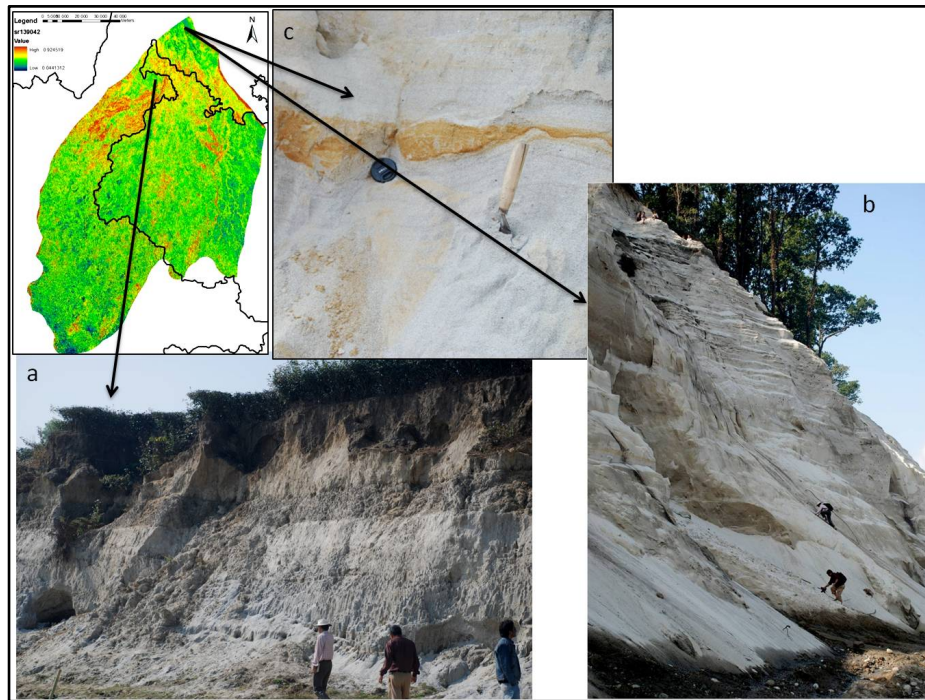


Figure 9: Photographs of deposits in the proximal portions of the DFS. a. well drained soil with sandy substrate beneath a tea plantation; b. the incision bank next to the Tista River; c. close up of the sandy sediments in the incision bank.

In the field I noted that the proximal portion of the Tista had well-drained soils with sandy substrate at the (Figure 9a and 9c). In this area, tea plantations are very common (Figure 9a). Soils in the proximal portion of the DFS remain dry throughout most of the year. The medial part of Tista DFS has sandy-silty soil with mottling (Figure 10c and 10d). Rice, a crop that requires saturated soils, is grown during monsoon, when soils are wet, and pineapple, mustard and other vegetables that require well-drained soils are grown, or fields may remain fallow, across this portion of the DFS in summer and winter, when the soils are relatively dry (Figure 10a

and 10b). The distal portion of Tista DFS has wet and poorly-drained soils throughout the year (Figures 11a and 11c). Waterlogged areas, swamps and ponds are very common on the distal portion of the DFS (Figure 11b). Rice is grown here throughout the year.



Figure 10: Photographs from the medial Tista DFS. a. a mustard field located over seasonally well drained soils; b. a pineapple field over seasonally drained soils; c and d. mottled soils from the medial portion of the fan.

For range statistics, low range value implies less variability in the thermal signature, which indicates less seasonal variation in soil moisture content. Therefore, in proximal part of Tista DFS low range values indicate low variability of the thermal signature though well-drained dry soils have been observed here in the field (Figures 8 and 9a). These low range values most likely reflect the stable thermal signature throughout the year of the evergreen tea plantation and forests in this area (Figure 9a). The presence of well-drained sandy-silty soils with mottling in the medial part is in correlation with the high range values of this area (Figure 8, 10c and 10d) (Veneman 1976). In the distal part of the DFS, soils are found to be poorly drained and wet, as expected from the low range values in this area (Figures 8, 11a and 11c).



Figure 11: Photographs from the Distal Tista DFS, showing gleyed soils (a and c) and waterlogged areas (b).

4.2 Kosi and Gandak DFSs

Image analyses of the Kosi and Gandak DFS present consistent relatively low range

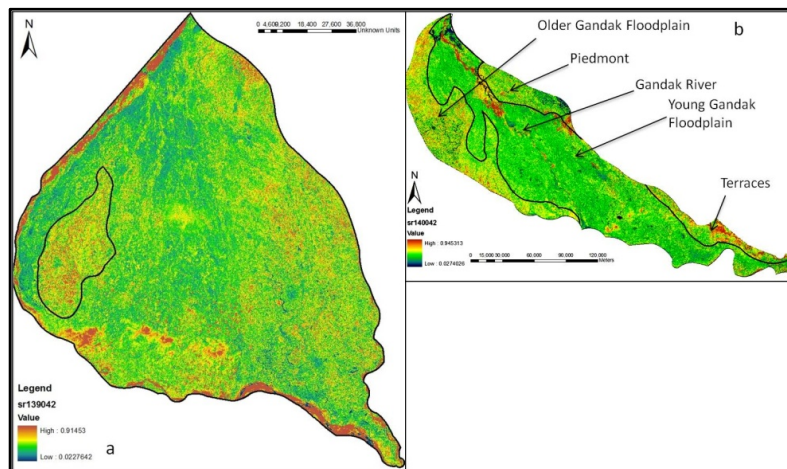


Figure 12: Range statistics for the Kosi DFS (a) and the Gandak DFS (b). Note the slightly raised area on the western Kosi DFS shows higher range values. On the Gandak DFS, the older Gandak Floodplain, Piedmonts, and terraces show higher range values whereas the Young Gandak Floodplain displays low range values. The geomorphic subdivisions on the Gandak DFS are from Pati et al. (2011) (see Figure 5).

values throughout these DFS surfaces with the exception of some scattered zones that display high thermal signal variability (Figures 12a and 12b). On Kosi DFS, cross-profile of SRTM

images show that these areas are relatively elevated (Figure 13). Thus, the water table is deeper in these elevated regions (Singh 1989) and thus seasonal variation in soil moisture content is high.

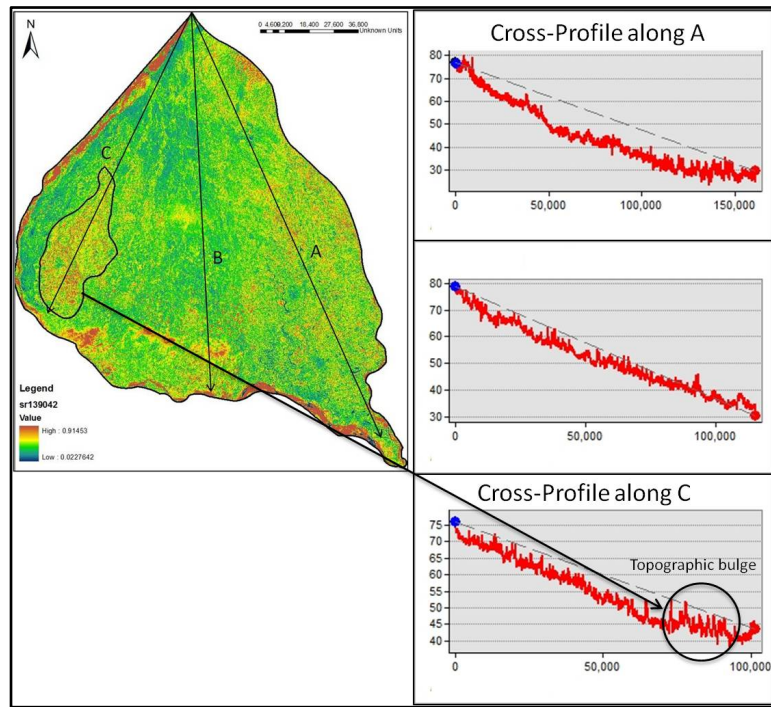


Figure 13: Three cross-profiles were drawn on SRTM images of Kosi DFS along A, B and C lines. Topographic height decreases almost constantly downstream. There is a topographic bulge in cross-profile along C that corresponds with high range value.

On Gandak DFS, high range values are seen on the Old Gandak Plain (Figure 12b). The Dartmouth Floodmap (Figure 14) shows that past floodwater are mostly confined in the Young Gandak Plain, indicating that the Old Gandak Plain is now detached from the main Gandak River and thus seasonal variation in moisture content is high here (Mohindra et al. 1992) (Figure 14).

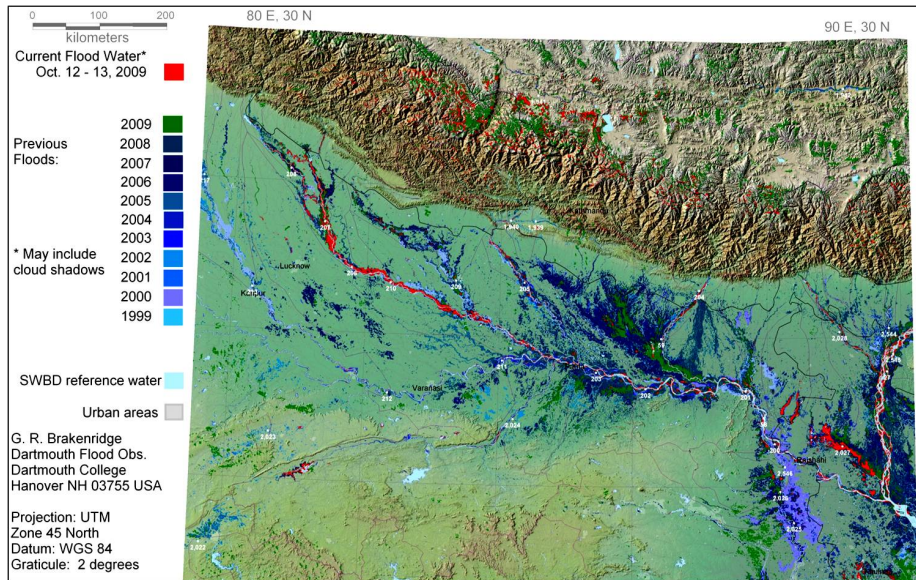


Figure 14: The Dartmouth Floodmap (<http://www.dartmouth.edu/~floods/hydrography/E80N30.html>) showing flooding patterns between 1999 and 2009 for the study area. On the Kosi DFS, flooding occurred across many parts of the DFS. On the Gandak DFS, floodwater is confined within the Young Gandak Floodplain. On the Ghaghra-Rapti incised DFS, floodwater is confined within the active and incised channelbelt.

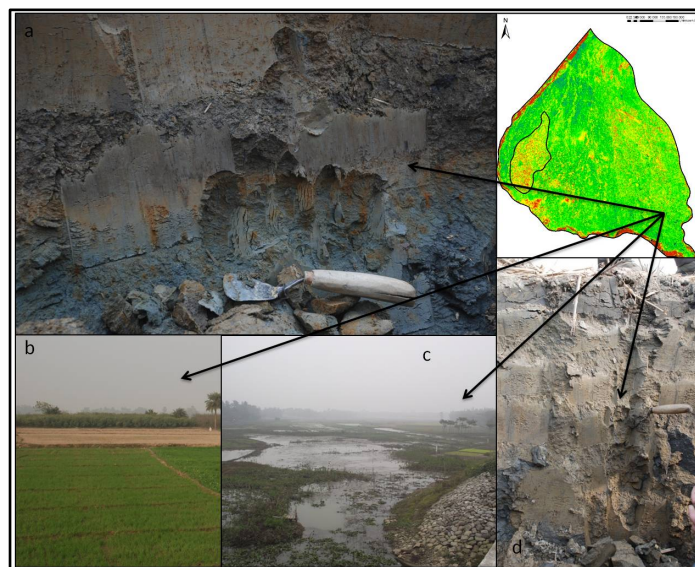


Figure 15: Photographs of soils and landscape on the distal Kosi DFS. a. Clay rich soils showing gleyed character above shallow water table (the water table lies just below the bottom of this profile). b. rice crops along the distal DFS; c. waterlogged areas and raised roadways; d. clay-rich, poorly drained soils.

The low range values displayed on these DFSs implies less variable thermal signal. Thus, I interpret that relatively poorly drained, wetter soils occur throughout these DFSs. In the field, I observed poorly drained clay-rich mottled soils in the distal part of the Kosi DFS, thus supporting this interpretation of the image analyses (Figures 15a and 15d).

4.3 Ghaghra-Rapti River systems

Pati et al. (2010) subdivided the area around the Ghaghra and Rapti Rivers into seven regions, including the Piedmont zone, Rapti Floodplain, Rapti Terminal fans, Ghaghra-Rapti interfluvium, Old Ghaghra Plain, the Ghaghra Floodplains, and the Ghaghra terraces (Figures 5 and 16a). In this study the outlines of these zones have been expanded based on the satellite imagery and the terminal fans have been included in the Ghaghra-Rapti interfluvium region (Figure 16b). Low range values are primarily confined to the Ghaghra

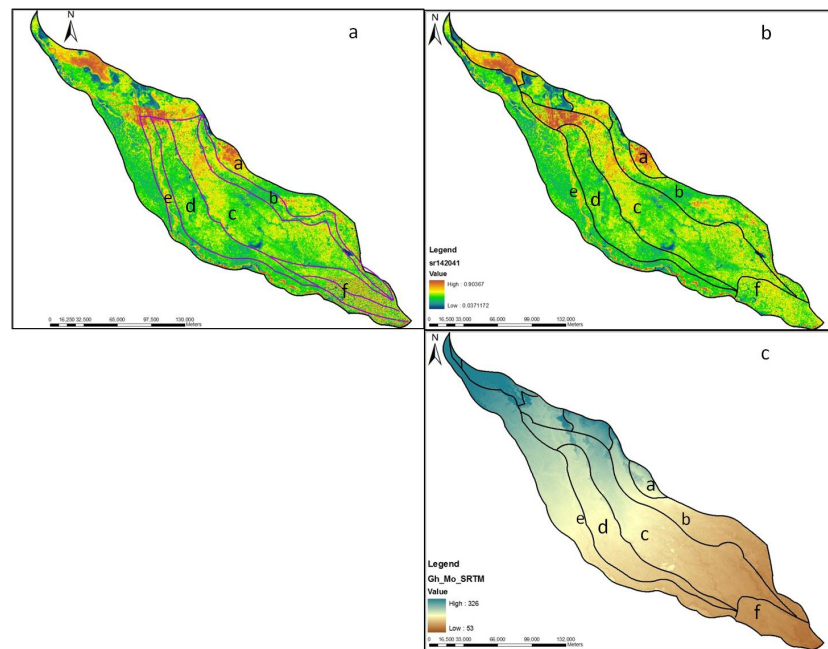


Figure 16: Range statistics (a and b) and SRTM elevation DEM (c) of the Ghaghra DFS. Subdivisions on (a) are from Pati et al (2011), and subdivisions on (b) and (c) are modified for this report. The subdivision symbols are: a - piedmont zone; b - Rapti Floodplain; c – Rapti-Ghaghra interfluvium region; d – Old Ghaghra floodplain; e - Ghaghra Plain; f - Terraces

floodplain area (Figure 16b). Rapti floodplain has low range values in its medial reaches, however it shows relatively high range values in the proximal and distal portions of the floodplain (Figure 16b). The abandoned Ghaghra floodplain, Ghaghra terraces and the proximal part of the interfluvium area display high range values (Figure 16b). The range value decreases in the distal portions of interfluvium area. These low range values are mostly aligned with areas that show

flooding on the Dartmouth floodmap (<http://www.dartmouth.edu/~floods/hydrography/E80N30.html>) (Figure 16b).

SRTM images of this area show that Ghaghra River is incised to a greater degree into its floodplain compared to Rapti (Figure 16c). In the Rapti River the degree of incision decreases downstream (Figure 16c). The upper part of the interfluvial area is highly elevated compared to the two floodplains of Ghaghra and Rapti. However, this difference decreases downstream (Figure 16c). The high range values on piedmont zones, Old Ghaghra Plain and Ghaghra terraces are probably due to their high elevation (Figures 16b and 16c).

In the elevated areas I generally observe high range values. Due to deeper water table, the soils in these areas are better drained and are dry throughout much of the year, except during monsoons when they become wet, thus producing the high range signal observed.

The Ghaghra River is incised and thus floodwater remains confined here and the water table is shallow in the Ghaghra River floodplain (Figures 14 and 16b). Therefore soils in this area remain wet throughout the year. This explains occurrence of low range values in the Ghaghra floodplain (Figure 16b). However on Rapti floodplain low range values can be found only in the middle part (Figure 16b). The floodmap shows that floodwater is not confined in the medial part of this floodplain and according to SRTM images its degree of incision decreases downstream (Figures 14, 16b and 16c). Thus, soils in the middle part remain wetter than those of the proximal DFS, reflecting in the range statistics with lower values (Figure 16b).

Although degree of incision of Rapti River decreases downstream, high range values are present in the distal part (Figure 16b and 16c). Field data are required to explain this observation. In the interfluvial area, due to decreasing elevation, water table depth decreases. Therefore I observe a downstream decrease in range values that indicate increasing soil moisture content down-dip similar to Tista DFS (Figures 8 and 16b).

5. DISCUSSION

Hartley et al. (*in press*) showed that soil moisture variations along three DFSs from three different continents are similar. Weissmann et al. (*in press*) showed three examples from the sedimentary rock record in which the vertical sedimentary succession display a general coarsening-upward succession of facies that consists of wetland deposits of the distal DFS toe overlain by sediments displaying well drained soils. They hypothesized that this succession has been resulted due to progradation of DFS.

This study, however, indicates that the variation of soil moisture in the Ganges basin is potentially more complex. In the current study, I analyzed soil moisture distribution on four river systems that are different from each other in terms of their depositional regime and degree of incision though all of them are situated in the same basin. This study indicates that the Tista DFS and the interfluvial area of Ghaghra-Rapti River system both of which are presently incised, shows the succession indicated by Hartley et al. (*in press*) and Weissmann et al. (*in press*) (Figures 8 and 16b). The Kosi and Gandak DFSs do not appear to fit in this trend (Figures 12a and 12b). They lie in regions of higher subsidence rate (Pati et al. 2010). Therefore, these DFS have not filled their accommodation space and thus they are not incised. The precise reasons behind this variation in distribution pattern in these river systems are not clear from this study. However, field observations along with literature survey have enabled us to identify that degree of DFS incision, which in turn is related to depth of groundwater, may be an important factor in controlling soil moisture distribution on the DFS.

5.1 Degree of incision:

A net aggradational setting in the eastern part of the Ganges foreland basin has been postulated, which has prompted the formation of the DFSs in the Himalayan Foreland Basin (Chakraborty et al. 2010c). However, deep river incision, presence of narrow, highly sinuous and underfit nature

of modern channels on the Tista DFS imply a net degradational setting under current climatic settings (Chakraborty et al. 2010c). Similarly, in the Ghaghra-Rapti river system both Ghaghra and Rapti Rivers are incised into their DFS (Pati et al. 2011). Currently they are not aggrading on the interfluvial area. In contrast, the Kosi and Gandak DFS are not incised and relatively recent flooding (e.g., Holocene) has occurred on these DFS surfaces.

A prominent trend with decreasing soil moisture downstream has been observed on Tista as well as on Ghaghra-Rapti interfluvial area. Alternatively, the Kosi and Gandak DFSs are part of the Middle Gangetic Plain and are marked by higher subsidence rate and thus, aggrading depositional settings under current climatic conditions (Pati et al. 2010). Therefore, both of these areas are characterized by presence of wet soils throughout the DFSs and absence of any zonation unlike Tista and Ghaghra-Rapti River system.

5.2 Depth to Water Table:

On the incised DFSs, as in Tista and Ghaghra-Rapti interfluvial, at the proximal and medial part due to higher incision of the rivers, the water table is deep. During the monsoon season as water table rises, soils become wet. However, for the rest of the year these well-drained soils remain dry. This causes variability, which is reflected on the range statistics as high range values and on the crop patterns. Due to this seasonal variation, on the medial part of Tista DFS rice is grown only during monsoon when soil is wet otherwise, pineapple, mustard are grown or the field remain empty (Figures 10a and 10b). In the distal part, rivers are less incised and thus water table depth is low and the water table remains relatively shallow throughout the year. Therefore, low range values are found in the distal part (Figures 8 and 16b). Water logging, swamps and ponds were observed in distal part of Tista DFS (Figure 11b). Due to the presence of wet soils, people grow rice throughout the year.

On aggrading DFSs (e.g., the Kosi and Gandak DFS) the water table is relatively shallow and remains almost constant along the DFSs resulting low range values (Figures 12a and 12b). On the Kosi DFS, water logging is commonly found due to seepage condition caused by a gentle hydraulic gradient and a very low depth to water table (Singh 1989). Similar to the Kosi, most of the paleochannels on Gandak DFS are fed by groundwater as the water table is shallow in this region (Mohindra 1994). However, high range values can be found on these fans, mostly due to elevation differences (Figures 12a and 13a). On the elevated areas where water table is deeper, dry, relatively well-drained soils are found. On the Gandak DFS, the old Gandak plain has dry soils as this area is elevated compared to the rest of the DFS (Figures 12b and 13b). Similarly on the Kosi near the western boundary of the DFS there is a zone of high elevation, which has dry soils (Figures 12a and 13a).

5.3 Climate

Precipitation increases by 100cm from west to east across the study area (Pati et al 2010) (Figures 2a, b, and c). However, in this study, soil moisture distribution across the DFSs does not seem to be controlled by climate. The study area is mostly in a wet climatic condition and therefore precipitation variability across the study area does not appear to play an important role in soil moisture distribution on these river systems. However, it should be noted that in a different climatic setting it might become important.

6. FUTURE WORK

It can be concluded from this study that Band 6 thermal images can be used for the study of soil moisture distribution across the DFSs in the Ganges basin. However, more rigorous fieldwork is

required in these DFSs to support these conclusions. The same methods should be applied on other DFSs located in different tectonic and climatic regimes.

7. CONCLUSIONS

1. The outcomes of this study show that thermal bands could be a useful tool for studying soil moisture content in this study area. The range statistics of thermal data appears to be reflecting relative water table depth, where deeper water table corresponds to relatively higher elevations of the soils versus the rivers, resulting in high range values.
2. Tista DFS and Ghaghra-Rapti interfluvium, which are currently incised, show a downstream increase in soil moisture content. On Tista DFS finer grain size, increasing presence of wetlands and changing crop pattern down the DFS reflect these soil moisture variability patterns.
3. On Kosi and Gandak DFS, which are in aggradational setting, there are wet soils throughout these DFSs and exceptional presences of dry soils are caused by elevation differences.
4. In the study area, soil moisture distribution on a DFS is controlled by the degree of river incision into the DFS and the water table depth.

Appendix I

There are two parts to the Appendix. In the first section methodology for different processes that have been used in this study have been discussed. Landsat and SRTM images were downloaded from (<http://glcfapp.glcg.umd.edu:8080/esdi/index.jsp>). The time series data were downloaded from (<http://glovis.usgs.gov/>). ArcMap was used to make False Color Composite image (Figures A1a-d), made with all seven Landsat bands, calculate range statistics of the time series with Landsat Band 6 data (Figures A2a-d), and classify the same time series using Maximum Likelihood classifier. In order to process the images as mentioned above after downloading all data were trimmed. After trimming the images used in Time series were extracted and standardized. These processes have also been described below. The MODIS data were obtained from (http://daac.ornl.gov/cgi-bin/MODIS/GLBVIZ_1_Glb/modis_subset_order_global_col5.Pl) and analyzed using a MATLAB code.

A2. DETAIL METHODOLOGY

Trimming

- Open uncompressed and trimmed file in ArcMap
- Run the following command in Spatial analyst toolbox (`[raster file]>0, [raster file]`)
- Save the resultant file
- Goal – The goal of trimming is to remove No-data from the downloaded satellite imageries (Figure A3.a and A3.b)

Making False Color Composite Image

- Toolbox – Data Management – Raster – Raster Processing – Composite bands
- Input – 7 bands

- Figures A1a-A1d

Making a Polygon

- Make a new .shp file in ArcCatalog
- Feature type – polygon
- Add new .shp file in ArcMap
- Start editing using Editor tool

Extraction of Data

- Arc Toolbox – Spatial analyst – Extraction – Extraction by Mask
- Input file – raster dataset
- Input mask – polygon (.shp file)
- Figure A4a – A4b
- Goal – extract the required area

Standardization of raster data

- Extract Data using Polygon mask
- Convert raster to float (Spatial Analyst toolbox – Float – [raster file])
- Use the following command in Spatial Analyst tool box ((maximum value-[raster data])/((maximum value-minimum value)))
- Figures A4a-A4b
- Goal – the value range of all raster data is not equal. Due to standardization the value of each raster data will range between +1 to 0

Range Statistics

- Spatial Analyst Toolbox
- Cell Statistics – Input raster data – Select Range as the Overlay Statistics

Maximum Likelihood Classification with Majority Filter

- Iso Cluster
 - ⇒ Arc Toolbox – Spatial Analyst – Multivariate – Iso Cluster
 - ⇒ Input – Raster data
 - ⇒ Select number of class
 - ⇒ Output – a .gsg signature file
- Maximum Likelihood Classification
 - ⇒ Arc Toolbox – Spatial Analyst – Multivariate – Maximum Likelihood Classification
 - ⇒ Input – Raster data and signature file
 - ⇒ Output – Classified Image
- Majority Filter
 - ⇒ Spatial Analyst Toolbox – Neighborhood Statistics
 - ⇒ Input data – ML classified Image
 - ⇒ Statistics type – Majority
- Slope determination of SRTM images
 - ⇒ Spatial Analyst Toolbox – Surface analysis – Slope
 - ⇒ Input – SRTM image
- MODIS NDVI data analysis

The MODIS data used for NDVI analysis were downloaded from (http://daac.ornl.gov/cgi-bin/MODIS/GLBVIZ_1_Glb/modis_subset_order_global_col5.pl). In this website data can be obtained for a particular latitude-longitude with specified a 3 kilometer area (default option) to either side of the point. The downloaded data consists NDVI values of 625 MODIS NDVI cells recorded since 2000 till 2011 with 16 days interval. NDVI is a 250m product. Therefore in the selected window there would be 12 pixels to either side of the central pixel and dimension of each pixel would be 250m. The total area of the selected window is $3.25*3.25 \text{ km}^2$ i.e. 10.56km^2 . The values were obtained as an excel data sheet which were then used in the following MATLAB code to generate graphs (Figures A6a-f) to show the general annual trend of NDVI values in different areas. Different lines in those graphs represent annual variation in NDVI values for each of those 625 points.

Matlab Code - Used for analysis of NDVI MODIS data

```
% Plotting MODIS data (NDVI and Evapotranspiration) with time
% We will import data from XYZ to matlab

clear all
%[Book,txt,row] = xlsread('File name with location and extension');
% We are selecting only the numerical values from the excel datasheet
[Book,txt,row] = xlsread('File name with location and extension');
% We are making a separate matrix with day numbers. MODIS data are
taken at
% 8 days interval
Day_number = [1    17   33   49   65   81   97   113  129
145  161  177  193  209 ...
 225  241  257  273  289  305  321  337  353];
% we want to transform the NDVI values to the real value
Book1 = (Book*0.00001);
% We are making a "for loop"
% There are data for 10 years - i=9
% Year_data - it consists data of a particular year
% in Year_data, when i=1 it will take all the numeric values from 1st
row
% to 46th row
% in Year_data, when i=2 it will take all the numeric values from 47th
row
% to 92nd row i.e. the values of next year
% In the graph Day_number will be in the x-axis and Year_data will be
in
% the Y-axis
% We have transposed Day_number.
% to make all lines black - figure; plot(Day_number', Year_data,'k')

for i = 1:11
    Year_data = zeros(23,625);

    Year_data(:, :) = Book1(1+(i-1)*23:23+(i-1)*23, :);

    figure; plot(Day_number', Year_data)
    title('NDVI versus time', 'FontSize', 14)
    xlabel('Time', 'FontSize', 12);
    ylabel('NDVI', 'FontSize', 12);

end
```

List of Reference

- Benito, M., Delahorra, R., Barrenechea, J., Lopezgomez, J., Rodas, M., Alonsoazcarate, J., Arche, a, et al. (2005). Late Permian continental sediments in the SE Iberian Ranges, eastern Spain: Petrological and mineralogical characteristics and palaeoenvironmental significance. *Palaeogeography, Palaeoclimatology, Palaeoecology*, 229(1-2), 24-39. doi:10.1016/j.palaeo.2004.12.030
- Bridge, J. S. (2003). *Rivers and Floodplains: Forms, Processes, and Sedimentary Record* (p. 504). Wiley-Blackwell. Retrieved from <http://www.amazon.com/Rivers-Floodplains-Processes-Sedimentary-Record/dp/0632064897>
- Carlson, T. N. (1994). A method to make use of thermal infrared temperature and NDVI measurements to infer surface soil water content and fractional vegetation cover.
- Carlson, T. N., Perry, E. M., & Schmugge, T. J. (1990). Remote estimation of soil moisture availability and fractional vegetation cover for agricultural fields. *Area*, 52, 45-69.
- Chakraborty, T., & Ghosh, P. (2010a). The geomorphology and sedimentology of the Tista megafan, Darjeeling Himalaya: Implications for megafan building processes. *Geomorphology*, 115(3-4), 252-266. Elsevier B.V. doi:10.1016/j.geomorph.2009.06.035
- Chakraborty, T., Kar, R., Ghosh, P., & Basu, S. (2010b). Kosi megafan: Historical records, geomorphology and the recent avulsion of the Kosi River. *Quaternary International*, 227(2), 143-160. Elsevier Ltd and INQUA. doi:10.1016/j.quaint.2009.12.002
- Gupta, S. (1997). Himalayan drainage patterns and the origin of fluvial megafans in the Ganges foreland basin. *Geology*, 25(1), 11-14.
- Collinson, J.D., 1996. Alluvial sediments. In: Reading, H.G. (Ed.), *Sedimentary Environments: Processes, Facies and Stratigraphy*. Blackwell Science, Cambridge, USA, pp. 37–82.
- De La Horra, R., Benito, M. I., López-Gómez, J., Arche, A., Barrenechea, J. F., & Luque, Javier. (2008). Palaeoenvironmental significance of Late Permian palaeosols in the South-Eastern Iberian Ranges, Spain. *Sedimentology*, 55(6), 1849-1873. doi:10.1111/j.1365-3091.2008.00969.x
- Decelles, P.G., Cavazza, W., 1999. A comparison of fluvial megafans in the Cordillarians (Upper Cretaceous) and modern Himalayan foreland basin systems. *Bulletin, Geological Society of America* 111, 1315–1334.

- Driese, S. G., Orvis, K. H., Horn, S. P., Li, Z.-H., & Jennings, D. S. (2007). Paleosol evidence for Quaternary uplift and for climate and ecosystem changes in the Cordillera de Talamanca, Costa Rica. *Palaeogeography, Palaeoclimatology, Palaeoecology*, 248(1-2), 1-23. doi:10.1016/j.palaeo.2006.11.013
- Duff, P.Mcl.D. (Ed.), 1992. Holmes' Principles of Physical Geology. Chapman and Hall, London, p. 789.
- Gohain, K., Prakash, B., 1990. Morphology of the Kosi Megafan. In: Rachoki, A., Church, M. (Eds.), Alluvial Fans: a Field Approach. John Willey and Sons Ltd, Chichester, UK, pp. 151–178.
- Gole, C.V., Chitale, S.V., 1966. Inland delta building activity of Kosi River. Journal of the Hydraulics Division, American Society of Civil Engineers 92 (HY2), 111–126.
- Gupta, S. (1997). Himalayan drainage patterns and the origin of fluvial megafans in the Ganges foreland basin. *Geology*, 25(1), 11-14.
- Hartley, a J., Weissmann, G. S., Nichols, G. J., & Warwick, G. L. (2010). Large Distributive Fluvial Systems: Characteristics, Distribution, and Controls on Development. *Journal of Sedimentary Research*, 80(2), 167-183. doi:10.2110/jsr.2010.016
- Hartley, A. J., Weissmann, Gary S, Bhattacharyya, P., Nichols, Gary J, Scuderi, L. A., Davidson, S. K., Leleu, S., et al. (in press). Soil development in modern sedimentary basins : implications for interpretation of paleosols in the rock record. *SEPM Special Publication*.
- Jain. V., Sinha. R., (2003), Hyperavulsive-anabranching Baghmata river system, North Bihar plains, eastern India., *Zeitschrift fur Geomorphologie*, 47(1), 101-116
- Jensen, J. R. (2006). *Remote Sensing of the Environment: An Earth Resource Perspective (2nd Edition)* (p. 608). Prentice Hall. Retrieved from <http://www.amazon.com/Remote-Sensing-Environment-Resource-Perspective/dp/0131889508>
- Joeckel, R. M. (1999). Paleosols in Gallesburg formation (Kansas city group, Upper Pennsylvanian), Northern Midcontinent, U.S.A.: Evidence for climate change and mechanisms of marine transgression., *Journal of Sedimentary Research*, 69(3), 720-737.
- Kleinert, K. (2001). Climate change in response to orographic barrier uplift : Paleosol and stable isotope evidence from the late Neogene Santa María basin , northwestern Argentina. *America*, (6), 728-742.

- Kraus, M. J. (1999). Paleosols in clastic sedimentary rocks: their geologic applications. *Earth-Science Reviews*.
- Mackey, S.D., Bridge, J.S., 1995. Three-dimensional model of alluvial stratigraphy: theory and application. *Journal of Sedimentary Research* 65, 7–31.
- May, J., Zech, R., & Veit, H. (2008). Late Quaternary paleosol–sediment-sequences and landscape evolution along the Andean piedmont, Bolivian Chaco. *Geomorphology*, 98(1-2), 34-54. doi:10.1016/j.geomorph.2007.02.025
- Miall, A. D. (1996). *The Geology of Fluvial Deposits: Sedimentary Facies, Basin Analysis, and Petroleum Geology* (p. 582). Springer. Retrieved from <http://www.amazon.com/Geology-Fluvial-Deposits-Sedimentary-Petroleum/dp/3540591869>
- Mira, M., Valor, E., Boluda, R., Caselles, V., & Coll, C. (2007). Influence of soil water content on the thermal infrared emissivity of bare soils: Implication for land surface temperature determination. *Journal of Geophysical Research*, 112(F4), 1-11. doi:10.1029/2007JF000749
- Mira, Maria, Caselles, Vicente, Valor, Enric, & Coll, César. (2009). Accurate assessment of land surface thermal emissivity. *Source*, (9), 187-193.
- Mira, Maria, Valor, Enric, Caselles, Vicente, Rubio, E., Coll, César, Galve, J. M., Niclòs, R., et al. (2010). Soil Moisture Effect on Thermal Infrared (8 – 13- μ m) Emissivity. *Measurement*, 48(5), 2251-2260.
- Mohindra, R., Prakash, B. (1994). Geomorphology and Neotectonic Activity of the Gandak Mega-fan and Adjoining areas, middle Gangetic Plains.
- Mookerjea, D., 1961. The Kosi—a challenge in river control. *Journal of Institution of Engineers (India)* 42, 117–142.
- Mookerjea, D., Aich, B.N., 1963. Sedimentation in the Kosi—a unique problem. *Journal of Institution of Engineers (India)* 43, 187–198.
- National Bureau of Soil Survey (NBSS) and Land Use Planning (LUP), 1992, Soils of West Bengal: Their kinds, distribution, characterization and interpretations for optimising land use: NBSS Publication 27, Soils of India Series 1.
- Pati. P., Prakash. B., Awasthi. A. K., Acharya. V., 2011 Holocene tectono-geomorphic evolution of parts of the Upper and Middle Gangetic plains, India., *Geomorphology*, 128(3-4), 148-170

- Retallack, G. J. (2009). Greenhouse crises of the past 300 million years. *Geological Society of America Bulletin*, 121(9-10), 1441-1455. doi:10.1130/B26341.1
- Ritter, D. F., Kochel, R. C., & Miller, J. R. (2006). *Process Geomorphology* (p. 560). Waveland Pr Inc. Retrieved from <http://www.amazon.com/Process-Geomorphology-Dale-F-Ritter/dp/1577664612>
- Shaw, J. A., Marston, C., (2000), Polarized infrared emissivity for a rough water surface., *Optics Express.*, 7(11)., 375-380
- Sheldon, N. D., & Tabor, N. J. (2009). Quantitative paleoenvironmental and paleoclimatic reconstruction using paleosols. *Earth-Science Reviews*, 95(1-2), 1-52. Elsevier B.V. doi:10.1016/j.earscirev.2009.03.004
- Singh, P. N., 1989, Ground water flow in southern part of Kosi alluvial fan and its effect on waterlogging with possible remedial measures, district saharas, Bihar, India,
- Singh, H., Parkash, B., Gohain, K., 1993. Facies analysis of the Kosi megafan deposits. *Sedimentary Geology* 85, 87–113.
- Sinha, R., & Friend, P. F. (1994). River systems and their sediment flux , Indo-Gangetic plains , Northern Bihar , India. *Sedimentology*, 41, 825-845.
- Sinha, R., Jain, V., Babu, G., & Ghosh, S. (2005). Geomorphic characterization and diversity of the fluvial systems of the Gangetic Plains. *Geomorphology*, 70(3-4), 207-225. doi:10.1016/j.geomorph.2005.02.006
- Sinha, R., Tandon, S. K., Gibling, M. R., Bhattacharjee, P. S., & Dasgupta, A. S. (2005). Late Quaternary geology and alluvial stratigraphy of the Ganga basin. *Himalayan Geology*, 26(1), 223-240.
- Tandon, S. K., Gibling, M. R., Sinha, R., Singh, V., Ghazanfari, P., Dasgupta, A., Jain, M., et al. (2006). Alluvial valleys of the Ganga Plains, India; timing and causes of incision.
- Veneman. P.L.M., Vepraskas. M. J., Bouma. J., 1976. The physical significance of soil mottling in a wisconsin toposequence., *Geoderma.*, 15., 103-118
- Wang, H., Li, X., Long, H., Xu, X., & Bao, Y. (2010). Catena Monitoring the effects of land use and cover type changes on soil moisture using remote-sensing data : A case study in China ' s Yongding River basin. *Area*, 82, 135-145. doi:10.1016/j.catena.2010.05.008

- Weissmann, G.S., Hartley, a J., Nichols, G.J., Scuderi, L. a, Olson, M., Buehler, H., & Banteah, R. (2010). Fluvial form in modern continental sedimentary basins: Distributive fluvial systems. *Geology*, 38(1), 39-42. doi:10.1130/G30242.1
- Weissmann, G.S., Hartley, A.J., Scuderi, L.A., Nichols, G.J., Davidson, S.K., Atchley, S.C., Bhattacharyya, P., Chakraborty, T., Ghosh, P., Nordt, L.C., Owen, A., and Sheldon, N., 2012, *Prograding Distributive Fluvial Systems – Geomorphic Models and Ancient Examples*, New Frontiers in Paleopedology and Terrestrial Paleoclimatology: SEPM Special Publication, Prograding Distributive Fluvial Systems – Geomorphic Models and Ancient Examples (in press)
- Wells, N.A., Dorr, J.A., 1987. Shifting of the Kosi River, northern India. *Geology* 15, 204–207.
- White, P. D., & Schiebout, J. (2008). Paleogene paleosols and changes in pedogenesis during the initial Eocene thermal maximum: Big Bend National Park, Texas, USA. *Geological Society of America Bulletin*, 120(11-12), 1347-1361. doi:10.1130/B25987.1
- Zhiming, Z., Qiming, Q. I. N., Abduwasit, G., & Dongdong, W. (2007). NIR-red spectral space based new method for soil moisture monitoring. *Construction*, 50(2001), 283-289. doi:10.1007/s11430-007-2004-6